ELSEVIER

Thermochimica Acta 307 (1997) 127–134

thermochimica acta

Synthesis and thermal behaviour of pentamethylcyclopentadienylrhodium(III) complexes with anilines

Gregorio Sánchez*, Joaquín García, José Pérez, Gabriel García, Gregorio López

Departamento de Química Inorgánica, Campus Universitario de Espinardo, Universidad de Murcia, 30071 Murcia, Spain

Received 10 May 1997; accepted 27 June 1997

Abstract

The complex $[RhCp^*Cl(\mu\text{-}Cl)]_2$ ($Cp^* = C_5Me_5$) reacts with RNH_2 (R = C_6H_5, p-$CH_3C_6H_4$, p-$CH_3OC_6H_4$, p-ClC_6H_4 and p-BrC_6H_4) in dichloromethane to form the corresponding pentamethylcyclopentadienylrhodium(III) derivatives $[RhCp^*Cl_2(RNH_2)]$. The compounds have been characterized by C, H and N analyses and spectroscopic methods (IR and ^1H NMR). The TG, DTG and DSC study of the complexes was carried out in both dynamic nitrogen and air atmospheres. From the DSC curves the heat of decomposition was calculated. The kinetics of the first step of thermal decomposition were evaluated from TG data by means of Coats–Redfern, MacCallum–Tanner and Horowitz methods and the procedure proposed by Dollimore et al. The values of the activation energy, E_a, and the pre-exponential factor, A, of the thermal decompositions were calculated. © 1997 Elsevier Science B.V.

Keywords: Pentamehtylcyclopentadienyl complexes; Rhodium; Thermal behaviour

1. Introduction

The chloro-bridged binuclear complex $[RhCp^*Cl(\mu\text{-}Cl)]_2$ ($Cp^* = C_5Me_5$) has been extensively used as a precursor in the synthesis of mononuclear complexes of the types $[RhCp^*Cl_2L]$ and $[RhCp^*ClL_2]^+$ (L = neutral ligand) [1–6]. Curiously, besides the synthesis of $[RhCp^*Cl_2$ (p-toluidine)] [1], there has not been an earlier study of aniline derivatives for the pentamethylcyclopentadienylrhodium(III) system. Thermal studies on pentamethylcyclopentadienylrhodium(III) derivatives with *N*-donor ligands such as pyridines and diamines have been previously reported [7]. Thermogravimetric data of these complexes showed the relatively great thermal stability of the chloro-bridged rhodium complex.

Here we report the preparation, characterization and thermal study of pentamethylcyclopentadienylrhodium(III) derivatives with some monodentate aromatic amines.

2. Experimental

The aromatic amines and pentamethylcyclopentadiene were obtained from commercial sources. The complex $[RhCp^*Cl(\mu\text{-}Cl)]_2$ was prepared by published methods [1]. The solvents were dried by conventional methods.

*Corresponding author. Tel.: 00 34 968 307100; fax: 00 34 68 36 41 48.

PII S0040-6031(97)00315-8

2.1. Preparation of the complexes

The complexes $[RhCp^*Cl_2(RNH_2)]$ were obtained by reaction of the dinuclear complex $[RhCp^*Cl(\mu\text{-}Cl)]_2$ with the corresponding aromatic amines in CH_2Cl_2 solution according to the following general method: The neutral ligand (aniline, *p*-toluidine, *p*-anisidine, *p*-chloroaniline or *p*-bromoaniline, respectively; 0.32 mmol) in dichloromethane (5 ml) was added to a solution of $[RhCp^*Cl(\mu\text{-}Cl)]_2$ (0.16 mmol) in dichloromethane (10 ml). After 1 h of constant stirring, the resulting red solution was concentrated under reduced pressure. The addition of diethyl ether caused the formation of orange crystals, which were filtered off, washed with diethyl ether and air dried.

2.2. Characterization

The C, H and N analyses were performed with a Carlo Erba microanalyser. Conductivities were measured with a Crison 525 conductimeter. The IR spectra was recorded on a Perkin–Elmer 16F PC FT–IR spectrophotometer using Nujol mulls between polyethylene sheets and ^1H spectra on a Bruker AC 200E instrument.

$[RhCp^*Cl_2(C_6H_5NH_2)]$ (**I**). Orange crystals, yield 81%. Analysis: found (%): C, 47.5; H, 5.8; N, 3.6; calcd.: C, 47.8; H, 5.5; N, 3.5. Non-conductor in acetone. IR (cm^{-1}) (Nujol): 3300, 3194, 3148 (ν NH), 270, 252 (ν RhCl). ^1H NMR (δ) [solvent $CDCl_3$; reference $SiMe_4$]: 7.27 (m, 3H, C_6H_5), 7.04 (m, 2H, C_6H_5), 4.80 (s, 2H, NH_2), 1.40 (singlet, 15H, Cp^*).

$[RhCp^*Cl_2(p\text{-}CH_3C_6H_4NH_2)]$ (**II**). Orange crystals, yield 74%. Analysis: found (%): C, 49.0; H, 6.0; N, 3.6; calcd.: C, 49.1; H, 5.8; N, 3.4. Non-conductor in acetone. IR (cm^{-1}) (Nujol): 3312, 3294, 3194, 3146, 3102 (ν NH), 270, 252 (ν RhCl). ^1H NMR (δ) [solvent $CDCl_3$; reference $SiMe_4$]: 7.03 (m, 4H, C_6H_4), 4.70 (s, 2H, NH_2), 1.41 (singlet, 15H, Cp^*).

$[RhCp^*Cl_2(p\text{-}MeOC_6H_4NH_2)]$ (**III**). Orange crystals, yield 84%. Analysis: found (%): C, 47.4; H, 5.8; N, 3.3; calcd.: C, 47.2; H, 5.6; N, 3.2. Non-conductor in acetone. IR (cm^{-1}) (Nujol): 3282, 3194 (ν NH), 270, 252 (ν RhCl). ^1H NMR (δ) [solvent $CDCl_3$; reference $SiMe_4$]: 7.35 (d, 2H, C_6H_4), 6.85 (d, 2H, C_6H_4), 5.62 (s, 2H, NH_2), 1.41 (singlet, 15H, Cp^*).

$[RhCp^*Cl_2(p\text{-}ClC_6H_4NH_2)]$ (**IV**). Orange crystals, yield 77%. Analysis: found (%): C, 44.2; H, 4.9; N, 3.4; calcd.: C, 44.0; H, 4.8; N, 3.2. Non-conductor in acetone. IR (cm^{-1}) (Nujol): 3300, 3210, 3152, 3110 (ν NH), 270, 250 (ν RhCl). ^1H NMR (δ) [solvent $CDCl_3$; reference $SiMe_4$]: 7.16 (m, 4H, C_6H_4), 4.59 (s, 2H, NH_2), 1.39 (singlet, 15H, Cp^*).

$[RhCp^*Cl_2(p\text{-}BrC_6H_4NH_2)]$ (**V**). Orange crystals, yield 71%. Analysis: found (%): C, 40.1; H, 4.6; N, 2.8; calcd.: C, 39.9; H, 4.4; N, 2.9. Non-conductor in acetone. IR (cm^{-1}) (Nujol): 3214, 3112 (ν NH), 280, 242 (ν RhCl). ^1H NMR (δ) [solvent $CDCl_3$; reference $SiMe_4$]: 7.19 (d, 2H, C_6H_4), 6.73 (d, 2H, C_6H_4), 4.63 (s, 2H, NH_2), 1.45 (singlet, 15H, Cp^*).

2.3. Thermal analysis

Thermoanalytical data were obtained from TG, DTG and DSC curves. TG and DTG curves were recorded on a Mettler TA-3000 system provided with a Mettler TG-50 thermobalance and DSC curves were recorded on a DSC-7 Perkin–Elmer instrument. The atmospheres used in different experiments were a pure nitrogen flow (50 ml min^{-1}, TG and DSC) and an air flow (50 ml min^{-1}, TG). The heating rate was 5°C min^{-1} with a sample mass range of 4–6 mg.

3. Results and discussion

3.1. Thermal stability

The results of thermal analyses are summarised in Table 1 and the TG curves of the compounds are presented in Figs. 1 and 2. All complexes decompose in the same way, in both flowing air and nitrogen atmospheres, giving the binuclear rhodium complex $[RhCp^*Cl(\mu\text{-}Cl)]_2$ with the concomitant release of the neutral ligand according to Eq. (1)

The chloro-bridged binuclear complex can be isolated in every case and identified by IR and ^1H NMR spectroscopy. Subsequent decomposition of the chloro-bridged complex occurs in the temperature range given in Table 1, the final residues being metallic rhodium and carbonous in the nitrogen atmosphere or Rh_2O_3 in the air atmosphere.

Table 1
TG and DTG data for the neutral rhodium (III) complexes (under dynamic nitrogen and air atmosphere; heating rate 5°C min^{-1})

Complex	Step	Temperature range (°C)	DTG_{max} (°C)	Weight loss (%) Found (calc.)	Assignment	Enthalpy change (kJ/mol)
$[Cp^*RhCl_2PhNH_2]$ in N_2	1	120–176	170.5	23.4 (23.2)	$PhNH_2$	43.69
	2	263–460	315.0	43.7 (51.2)	$Cp^* + Cl_2$	
	Residue	>500	—	29.8 (25.6)	Rh + C	
$[Cp^*RhCl_2PhNH_2]$ in air	1	118–176	169.0	23.7 (23.2)	$PhNH_2$	
	2	251–402	286.0	42.0 (51.2)	$Cp^* + Cl_2$	
	Residue	>500	—	29.7 (31.6)	1/2 Rh_2O_3	
$[Cp^*RhCl_2(p\text{-}MeC_6H_4NH_2)]$ in N_2	1	101–171	164.5	24.6 (25.7)	p-$MePhNH_2$	36.06
	2	262–397	290.0	40.0 (49.5)	$Cp^* + Cl_2$	
	Residue	>500	—	29.4 (24.7)	Rh + C	
$[Cp^*RhCl_2(p\text{-}MeC_6H_4NH_2)]$ in air	1	116–179	171.5	24.5 (25.7)	p-$MePhNH_2$	
	2	251–401	284.0	47.8 (49.5)	$Cp^* + Cl_2$	
	Residue	>500	—	26.7 (30.5)	1/2 Rh_2O_3	
$[Cp^*RhCl_2(p\text{-}MeOC_6H_4NH_2)]$ in N_2	1	129–203	185.2	28.2 (28.5)	p-$MeOPhNH_2$	32.51
	2	278–402	298.0	44.0 (47.7)	$Cp^* + Cl_2$	
	Residue	>500	—	26.5 (23.8)	Rh + C	
$[Cp^*RhCl_2(p\text{-}MeOC_6H_4NH_2)]$ in air	1	137–197	185.2	26.8 (28.5)	p-$MeOPhNH_2$	
	2	232–405	279.0	43.6 (47.7)	$Cp^* + Cl_2$	
	Residue	>500	—	28.1 (29.4)	1/2 Rh_2O_3	
$[Cp^*RhCl_2(p\text{-}ClC_6H_4NH_2)]$ in N_2	1	123–188	180.5	31.6 (29.3)	p-$ClPhNH_2$	40.8
	2	278–458	312.5	37.3 (41.7)	$Cp^* + Cl_2$	
	Residue	>500	—	29.4 (23.6)	Rh + C	
$[Cp^*RhCl_2(p\text{-}ClC_6H_4NH_2)]$ in air	1	114–188	181.0	31.3 (29.3)	p-$ClPhNH_2$	
	2	262–410	289.5	35.5 (41.7)	$Cp^* + Cl_2$	
	Residue	>500	—	32.4 (29.1)	1/2 Rh_2O_3	
$[Cp^*RhCl_2(p\text{-}BrC_6H_4NH_2)]$ in N_2	1	135–192	179.5	35.8 (35.8)	p-$BrPhNH_2$	38.9
	2	270–418	311.0	34.8 (42.9)	$Cp^* + Cl_2$	
	Residue	>500	—	27.0 (21.4)	Rh + C	
$[Cp^*RhCl_2(p\text{-}BrC_6H_4NH_2)]$ in air	1	114–190	178.0	36.6 (35.8)	p-$BrPhNH_2$	
	2	272–396	289.5	32.0 (42.9)	$Cp^* + Cl_2$	
	Residue	>500	—	29.8 (26.4)	1/2 Rh_2O_3	

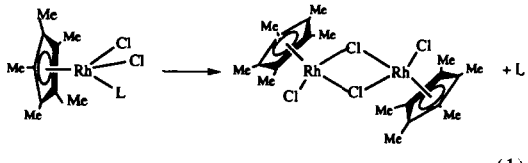

(1)

The enthalpy changes for the thermal decomposition processes were calculated by integration of the endothermic peaks in the corresponding DSC curves (Table 1).

3.2. *Recognizing the kinetic mechanism and kinetic parameters*

The models and expressions of functions for the most common mechanisms operating in solid-state decompositions, which have been tested in the present work, are listed in Table 2. The decomposition mechanism for the first step of the processes studied was evaluated from TG curves using the Coats–Redfern (CR), MacCallum–Tanner (MT) and Horowitz–Metzger (HM) methods. The following equations were used:

(a) The Coats–Redfern equation [8]:

$$\ln[g(\alpha)/T^2] = \ln[AR/\beta E_a(1 - 2RT/E_a)] - E_a/RT$$

(b) The MacCallum–Tanner equation [9]:

$$\log g(\alpha) = \log[AE_a/\beta R] - 0.485^{0.435} - [(0.449 + 0.217E_a) \times 10^3]/T$$

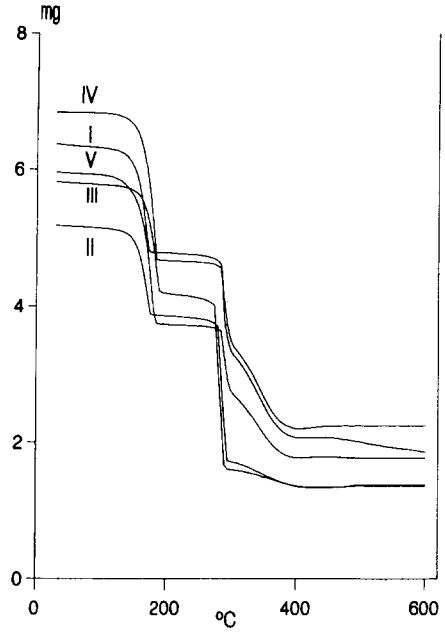

Fig. 1. TG curves of the rhodium complexes (in nitrogen).

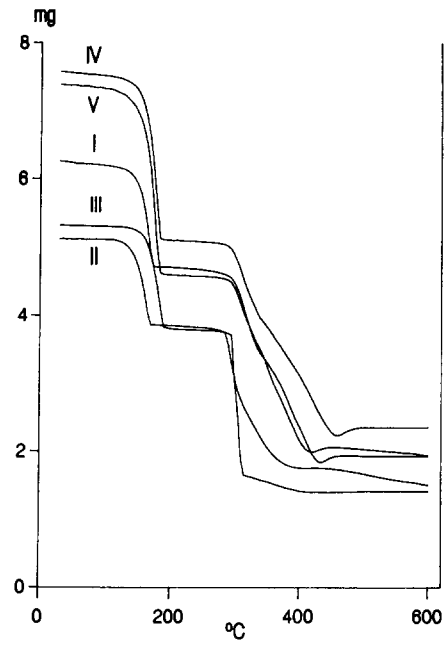

Fig. 2. TG curves of the rhodium complexes (in air).

(c) The Horowitz–Metzger equation [10]:

$$\ln g(\alpha) = \ln[AE_aT_s^2/\beta E_a] - E_a/RT_s + E_a\theta/RT_s^2$$

where α is the fraction of the sample decomposed at time t, $\theta = T - T_s$, T_s being the DTG peak temperature, β the heating rate, E_a the energy of activation, and A the pre-exponential factor. The kinetic parameters were calculated from the linear plots of the left-hand side of the kinetic equation against $1/T$ for Coats–Redfern and MacCallum–Tanner equations, and for Horowitz–Metzger equation the left-hand side is plotted against θ. The values of E_a and A were calculated, respectively, from the slope and intercept of the straight lines.

Values of the kinetic parameters and linear regression coefficients for the first stage of decomposition in both nitrogen and air atmospheres are listed in Table 3. The regression coefficients calculated for

Table 2
List of $f(\alpha)$ and $g(\alpha)$ functions

Mechanism	$f(\alpha)$	$g(\alpha)$
D_1	$1/2\alpha$	α^2
D_2	$-1/\ln(1-\alpha)$	$(1-\alpha)\ln(1-\alpha)+\alpha$
D_3	$(3(1-\alpha)^{2/3})/2[1-(1-\alpha)^{1/3}]$	$[1-(1-\alpha)^{1/3}]^2$
D_4	$3/2[1-(1-\alpha)^{-1/3}-1]$	$[1-(2\alpha/3)]-(1-\alpha)^{2/3}$
F_1	$1-\alpha$	$-\ln(1-\alpha)$
F_2	$(1-\alpha)^2$	$1/(1-\alpha)$
F_3	$(1-\alpha)^3/2$	$[1/(1-\alpha)]^2$
P_3	$2\alpha^{1/2}$	$\alpha^{1/2}$
$A_{1.5}$	$3/2(1-\alpha)[-\ln(1-\alpha)]^{1/3}$	$[-\ln(1-\alpha)]^{2/3}$
A_2	$2(1-\alpha)[-\ln(1-\alpha)]^{1/2}$	$[-\ln(1-\alpha)]^{1/2}$
A_3	$3(1-\alpha)[-\ln(1-\alpha)]^{2/3}$	$[-\ln(1-\alpha)]^{1/3}$
A_4	$4(1-\alpha)[-\ln(1-\alpha)]^{3/4}$	$[-\ln(1-\alpha)]^{1/4}$
R_2	$2(1-\alpha)^{1/2}$	$1-(1-\alpha)^{1/2}$
R_3	$3(1-\alpha)^{2/3}$	$1-(1-\alpha)^{1/3}$

Table 3
Kinetic parameters and correlation coefficients (r) calculated using Coats–Redfern (CR), MacCallun–Tanner (MT) y Horowitz–Metzger (HM) equations

Compound	Model	E_a (kJ mol^{-1})	log A	r	Method
I (in N_2)	R2	169.7	17.7	0.99965	CR
	D3	361.9	40.2	0.99960	
	D4	341.1	37.6	0.99960	
	R3	177.4	18.6	0.99959	
	R2	169.3	17.7	0.99968	MT
	D4	341.8	37.8	0.99962	
	R3	177.0	18.5	0.99962	
	D3	362.7	40.4	0.99962	
	R3	193.9	20.5	0.99960	HM
	D3	387.8	43.3	0.99960	
	R2	185.8	19.7	0.99942	
	D4	365.8	40.6	0.99926	
I (in air)	D1	249.6	27.4	0.99991	CR
	D2	271.5	29.9	0.99988	
	D4	280.3	30.3	0.99922	
	R2	138.9	14.0	0.99885	
	D1	249.7	27.5	0.99992	MT
	D2	271.7	30.0	0.99968	
	D4	280.5	30.4	0.99925	
	R2	138.3	13.9	0.99894	
	D2	294.3	32.6	0.99993	HM
	D4	303.6	33.2	0.99972	
	D1	271.0	30.0	0.99964	
	R2	154.3	15.9	0.99964	
II (in N_2)	D2	227.5	24.9	0.99993	CR
	D1	209.3	22.9	0.99971	
	D4	234.6	25.2	0.99969	
	R2	115.7	11.3	0.99946	
	D2	227.3	24.9	0.99993	MT
	D1	209.1	22.9	0.99974	
	D4	234.5	25.2	0.99970	
	R2	114.9	11.2	0.99950	
	D4	259.1	28.2	0.99993	HM
	D2	251.3	27.8	0.99991	
	R2	131.6	13.3	0.99986	
	R3	137.4	13.9	0.9995	
II (in air)	D2	275.2	30.2	0.99993	CR
	D4	285.3	30.8	0.99989	
	D1	250.4	27.4	0.99952	
	R2	141.8	14.3	0.99934	
	D2	275.5	30.3	0.99993	MT
	D4	285.7	30.9	0.99966	
	D1	250.6	27.4	0.99955	
	R2	141.3	14.2	0.99939	
	D2	298.1	32.9	0.99995	HM
	D4	308.9	33.6	0.99993	
	R2	157.4	16.1	0.99980	
	D3	330.8	36.4	0.99914	

Table 3 (*Continued*)

Compound	Model	E_a (kJ mol^{-1})	log A	r	Method
III (in N_2)	D3	311.4	32.9	0.99986	CR
	R3	152.0	14.8	0.99986	
	R2	144.9	14.1	0.99981	
	D4	292.2	30.6	0.99970	
	D3	312.2	33.1	0.99986	MT
	R3	151.8	14.7	0.99986	
	R2	144.6	14.0	0.99984	
	D4	292.8	30.7	0.99972	
	R3	168.4	16.7	0.99979	HM
	D3	336.8	35.8	0.99979	
	R2	160.9	16.0	0.99945	
	A1.5	123.1	11.9	0.99931	
III (in air)	R2	154.3	15.2	0.99992	CR
	D4	308.7	32.4	0.99990	
	D2	295.3	31.5	0.99948	
	D3	336.3	35.8	0.99940	
	R2	154.2	15.1	0.99993	MT
	D4	309.5	32.6	0.99991	
	D2	296.0	31.6	0.99951	
	D3	337.2	36.0	0.99942	
	R2	168.6	16.9	0.99980	HM
	D3	358.3	38.3	0.99971	
	R3	179.2	18.0	0.99971	
	D4	329.4	34.8	0.99960	
IV (in N_2)	D1	225.4	23.8	0.99996	CR
	D2	245.4	26.0	0.99923	
	D4	253.3	26.3	0.99857	
	R2	125.1	11.9	0.99803	
	D1	225.5	23.8	0.99996	MT
	D2	245.6	26.0	0.99927	
	D4	253.6	26.4	0.99864	
	R2	124.6	11.8	0.99821	
	D1	247.7	26.4	0.99990	HM
	D2	269.1	28.8	0.99979	
	D4	277.6	29.2	0.99941	
	R2	141.1	13.8	0.99911	
IV (in air)	D1	233.2	24.7	0.99997	CR
	D2	252.8	26.8	0.99953	
	D4	260.6	27.1	0.99901	
	R2	128.7	12.3	0.99858	
	D1	233.4	24.7	0.99997	MT
	D2	253.1	26.9	0.99955	
	D4	260.9	27.2	0.99905	
	R2	128.2	12.2	0.99870	
	D2	277.6	29.7	0.99987	HM
	D1	256.5	27.4	0.99971	
	D4	285.9	30.1	0.99961	
	R2	145.2	14.3	0.99938	

Table 3 (*Continued*)

Compound	Model	E_a (kJ mol^{-1})	log A	r	Method
V (in N_2)	D1	242.3	25.9	0.99993	CR
	D2	265.0	28.4	0.99934	
	D4	274.3	28.9	0.99867	
	R2	136.0	13.2	0.99811	
	D1	242.5	25.9	0.99993	MT
	D2	265.4	28.5	0.99937	
	D4	274.7	29.0	0.99872	
	R2	135.5	13.2	0.99827	
	D2	288.7	31.2	0.99981	HM
	D1	264.4	28.5	0.99978	
	D4	298.5	31.7	0.99942	
	R2	151.9	15.1	0.99911	
V (in air)	D1	192.8	20.1	0.99928	CR
	D2	211.0	22.1	0.99721	
	D4	218.3	22.3	0.99587	
	R2	107.5	9.9	0.99473	
	D1	192.7	20.1	0.99931	MT
	D2	210.9	22.1	0.99736	
	D4	218.3	22.4	0.99610	
	R2	106.8	9.8	0.99531	
	D1	214.7	22.7	0.99984	HM
	D2	234.3	24.8	0.99862	
	D4	242.3	25.2	0.99766	
	R2	123.3	11.8	0.99703	

the rhodium complexes show a good concordance between the results obtained by using Coats–Redfern and MacCallum–Tanner methods. However, the values of the linear regression coefficients do not allow to identify unambiguously the mechanism of the thermal decomposition of the complexes.

Dollimore et al. [11–13] have pointed out the significance of the onset and final temperatures, and α_{max} (α at the maximum reaction rate) in the kinetic analysis of TG curves. In this way, they have shown that the mechanism can be determined by considering the following parameters [13]: The diffuse or sharp character of the initial and final reaction temperature (T_i and T_f), the half-width, defined as the width on the differential plot of ($d\alpha/dT$) against T measured at the half-way point of the line drawn from the peak temperature perpendicular to the base line, and α_{max}.

In our study, all the TG plots of the complexes show (T_i) diffuse and (T_f) sharp (Figs. 1 and 2). The TG/DTG curves of the complexes [RhCp*Cl$_2$L], under nitrogen and air atmosphere, give an α_{max} between 0.78 and 0.84, corresponding to a D_2 mechanism [12].

The values of activation energy (E_a) and the pre-exponential factor (A), for the first step of the processes studied, have been obtained using the single-heating-rate differential (SHRD) method [14]:

$$\ln[(d\alpha/dt)/f(\alpha)] = \ln A - E_a/RT$$

A plot of $\ln[(d\alpha/dt)/f(\alpha)]$ vs. $1/T$ is obtained by feeding the experimental data. The activation energy and the pre-exponential factor can be calculated from the slope and intercept of the regression line obtained by regression analysis.

Dollimore suggests that the experimental TG and DTG curves can be reproduced using the Arrhenius parameters, together with the heating rate and kinetic equation [15]. We present in Table 4 a comparison between the theoretical parameters obtained from the reproduced curves (α_{max}, T_p, LoT, HiT and half width) and the experimental values. A high concordance should be noted.

Table 4
Parameters describing the asymmetry of the DTG curves for the first step of the thermal decomposition of the rhodium(III) complexes for D_2 mechanism (theoretical parameters in parentheses) and kinetic parameters calculated using SHRD method

Complex	α_{max}	T_p (°C)	LoT (°C)	HiT (°C)	Half width (°C)	$\Delta L_0 T/\Delta H_i T$	E_a (kJ mol^{-1})	log A
I (in N_2)	0.817	169.5	158.0	173.0	15.0	3.286	311.8	34.8
	(0.824)	(168.9)	(158.0)	(174.0)	(16.0)			
I (in air)	0.785	168.5	157.5	172.5	15.0	2.750	277.9	30.7
	(0.824)	(168.6)	(156.0)	(174.0)	(18.0)			
II (in N_2)	0.834	164.5	150.5	168.5	18.0	3.550	230.0	25.4
	(0.822)	(163.6)	(149.0)	(169.0)	(20.0)			
II (in air)	0.829	171.5	158.5	175.0	16.5	3.714	275.2	30.3
	(0.823)	(170.7)	(159.0)	(175.0)	(16.0)			
III (in N_2)	0.791	185.0	169.0	189.5	20.5	3.556	265.5	28.1
	(0.822)	(185.0)	(171.0)	(191.0)	(20.0)			
III (in air)	0.779	185.0	171.0	189.5	18.5	3.111	283.5	30.2
	(0.823)	(185.2)	(173.0)	(191.0)	(18.0)			
IV (in N_2)	0.799	180.5	169.0	184.5	15.5	2.875	258.4	27.6
	(0.823)	(180.4)	(166.0)	(186.0)	(20.0)			
IV (in air)	0.816	181.0	169.5	184.5	15.0	3.286	264.1	28.2
	(0.823)	(180.5)	(168.0)	(186.0)	(18.0)			
V (in N_2)	0.821	179.5	168.0	183.0	15.0	3.286	274.9	29.7
	(0.823)	(178.9)	(167.0)	(183.0)	(16.0)			
V (in air)	0.816	178.0	167.0	181.5	14.5	3.143	232.4	24.7
	(0.821)	(177.7)	(162.0)	(184.0)	(22.0)			

Acknowledgements

We thank the Consejería de Cultura y Educación de Murcia, Spain (project PCOM-17/96 EXP), for financial support.

References

[1] J.W. Kang, K. Moseley, P. Maitlis, J. Am. Chem. Soc. 91 (1969) 5970.
[2] W. Rigby, J.A. McCleverty, P. Maitlis, J. Chem. Soc., Dalton Trans., (1979) 382.
[3] F. Faraone, V. Marsala, G. Tresoldi, J. Organomet. Chem. 152 (1978) 337.
[4] D.S. Gill, P. Maitlis, J. Organomet. Chem. 87 (1975) 359.
[5] M.T. Youinou, R. Ziessel, J. Organomet. Chem. 363 (1989) 197.
[6] G. García, G. Sánchez, I. Romero, I. Solano, M.D. Santana, G. López, J. Organomet. Chem. 408 (1991) 241.
[7] G. Sánchez, I. Solano, M.D. Santana, G. García, J. Gálvez, G. López, Termochim. Acta 211 (1992) 163.
[8] A.W. Coats, P.J. Redfern, Nature 201 (1964) 68.
[9] J.R. MacCallum, J. Tanner, Eur. Polym. J. 6 (1970) 1033.
[10] H.H. Horowitz, G. Metzger, Anal. Chem. 35 (1963) 1964.
[11] D. Dollimore, T.A. Evans, Y.F. Lee, G.P. Pee, F.W. Wilburn, Thermochim. Acta 196 (1992) 255.
[12] X. Gao, D. Chen, D. Dollimore, Thermochim. Acta 223 (1993) 75.
[13] D. Dollimore, P. Tong, K.S. Alexander, Thermochim. Acta 282/283 (1996) 13.
[14] P.K. Heda, D. Dollimore, K.S. Alexander, D. Chen, E. Law, P. Bicknell, Thermochim. Acta 255 (1995) 255.
[15] D. Dollimore, T.A. Evans, Y.F. Lee, F.W. Wilburn, Thermochim. Acta 188 (1991) 77.